Hindawi
Advances in Civil Engineering
Volume 2019, Article ID 7953434, 10 pages
https://doi.org/10.1155/2019/7953434

Research Article

Research on Pressure Drop in the Accelerate Zone of Horizontal Conveying of Concrete Spraying

Guanguo Ma,[1] Zhaoxia Liu,[1] Xiaobing Gong,[1] Lianjun Chen,[1] Guoming Liu,[2] Gang Pan,[1] and Qizheng Dong[1]

[1]*College of Mining and Safety Engineering, Shandong University of Science and Technology, Qingdao 266590, China*
[2]*Chongqing Research Institute of China Coal Science and Industry Group, Chongqing 400016, China*

Correspondence should be addressed to Zhaoxia Liu; zhaoxialiu@163.com and Lianjun Chen; skyskjxz@163.com

Received 28 April 2019; Revised 17 July 2019; Accepted 25 July 2019; Published 23 December 2019

Academic Editor: Xu Yang

A pressure transmitter was installed at a specific position in a concrete conveying line to disclose the pressure drop when compressed air was conveyed during concrete spraying. A statistical analysis of the pressure at different positions was undertaken. Experimental results demonstrated that in the accelerate zone of horizontal conveying of concrete in the line, the pressure drop mainly occurred during the acceleration, collision, and friction processes. The momentum equation was introduced during the experiment, which interpreted the pressure drop caused by the accelerated conveying of concrete. The theoretical equation was corrected based on the results of theoretical experiments by introducing the value of α, and the experimental results were then optimized, thus obtaining an approximate model of pressure drop during the conveying of concrete. In addition, experimental results were compared with a model equation that showed the reliability of the proposed model. Research conclusions are of great significance to regulate the pressure drop in the conveying line of concretes, to design working parameters of concrete spraying devices, and to predict the ultimate distance for the conveying of concrete.

1. Introduction

Concrete spraying technology is extensively applied in underground projects (e.g., railway and tunnel) and tunnel construction in coal mines in China [1–3]. Because of its associated conveniences, wind-driven concrete spraying technology has been widely applied. Concrete spraying is a process that conveys stirred concrete in a closed line by compressed air to the nozzle and is then sprayed, which is the process of pneumatic conveying. However, the conveying process of concrete is relatively complicated, and it lacks theoretical references related to the prediction of concrete conveying distance. Instead, generally, the concrete conveying distance can only be estimated. Therefore, it is necessary to study the process and mechanism of wind-driven concrete conveying. Research results provide theoretical references for the design of a shotcrete machine and prediction of the conveying distance.

Pressure drop should be considered in the design of a concrete conveying system. When calculating the pressure drop in delivery lines, the classic phase diagram is often applied, in which the pressure drop in unit length of the line is expressed as a function related to speed [4, 5]. Forces in concrete and on the pipe walls predict the pressure drop in the conveying of concrete. Naveh et al. showed the effect of the slip velocity of particles on pressure drop by studying the pressure drop during the pneumatic transmission of various types of particles. These authors believed that understanding the velocity of particles in the steady-state region was vital for reliably designing the entire conveying process [6]. Brown showed that the flow of particles and fluid were the primary causes of pressure drop during pneumatic transmission and constructed a linear equation to express pressure drop during the velocity stabilization zone [7], and it can be described as

$$\Delta P_{ss} = \Delta P_c + \Delta P_f, \quad (1)$$

where ΔP_{ss} is the constant pressure drop, ΔP_c is the pressure drop caused by concrete, and ΔP_f is the pressure drop caused by compressed air.

Here,

$$\Delta P_f = f_D \frac{\rho_f u_f^2}{2D} L, \quad (2)$$

where f_D is the coefficient of friction in pipe, ρ_f is the density of compressed air, u_f is the air velocity, D is the internal diameter of the pipeline, and L is the conveying distance.

Conveying concrete using the driving effect of compressed air exists in a suspension flow state. Because of the high fluid velocity, the influences of gravity on the state of conveying can be neglected [8–10]. At the start of conveying, concrete is conveyed into the line by a shotcrete machine at zero velocity under the action of compressed air. Momentum is transferred from air to concrete and can trigger disturbance of air flow as well as changes in momentum. Air pressure is needed during this process and is significantly higher than that required during single-phase flow [11–13]. Therefore, the accelerated conveying of concrete in line requires an accelerate zone that refers to the process from the beginning of the accelerated conveying of concrete to the stable conveying speed [14].

In the present study, the pressure drop caused by accelerated conveying of concrete is considered. During the conveying of concrete, the pressure drop in the accelerate zone is mainly attributed to acceleration, collision, and friction of concrete. The acceleration of concrete only occurs in the accelerate zone, whereas collision and friction occur throughout the conveying of concrete. The total pressure drop in the accelerate zone can be defined as the sum of the steady-state pressure drop and accelerated pressure drop [8]. The pressure drop caused by acceleration must be first considered when analyzing the pressure drop in the horizontal accelerate zone of concrete transfer. The pressure drop caused by acceleration is generally determined by pressure distribution in the accelerate zone. The accelerate zone from the shotcrete machine to the nozzle is mainly distributed under two situations: the first accelerate zone is called the initial accelerate zone when concrete and compressed air begin to flow. The second accelerate zone is the region after the concrete passes through the bent pipe. Studying the law of pressure drop in the accelerate zone of concrete has great significance for predicting the conveying distance of concrete [15, 16].

Many researchers have proven that the pressure drop caused by concrete friction and collision in the steady-state region was different from that in the accelerate zone. Hence, the pressure drop in the accelerate zone cannot be predicted by the momentum equation of concrete and is often predicted by the correlation between concrete collision and friction during the conveying process [17–20].

Ottjes has researched the movement of the particle in horizontal pipes, which took the lifting force of materials and the inelastic collision between particles and pipe wall into account [21]. Nguyen analyzed the movement of single particles in horizontal pipelines, especially considering the effect of Magnus [22]. Huber and Sommerfeld conducted a three-dimensional numerical simulation of the dilute phase flow pneumatic transport and predicted the particle distribution in horizontal pipelines and 90-degree bent pipes by considering two-way coupling, turbulence, and the dispersion law of turbulent particles [23].

Hanley et al. proposed a method based on process randomness to quantify particle collision in the line that can be used to express the pressure drop caused by the collision of internal aggregates during the acceleration process [24]. Klinzing and Basha studied variations in average particle speed based on abundant experimental data and constructed a correlation, providing reasonable theoretical references for the conveying of concrete under the effect of compressed air [25]. Merkus and Meesters proposed a method to describe the pressure drop during the acceleration process using the momentum equation. They expressed the variation equation of concrete particles and air momentum and proposed a method to predict the pressure drop in acceleration. However, they did not construct an appropriate pressure drop model in the accelerate zone, thus failing to judge the accuracy of the pressure drop curve in the accelerate zone [26].

The present study focused on studying the law of pressure drop in the accelerate zone of the pneumatic transmission of concrete. This was to study the relationship between the variation law of the momentum of air and concrete particles and the pressure drop in the accelerate zone. The air-concrete ratio was changed by altering the flow rate of compressed air and the supply quantity of concrete. In addition, the input pressure of compressed air was changed. Pressure changes in the line were measured by a pressure transmitter. A mathematical model was constructed to analyze the law of pressure drop in the accelerate zone of pneumatic transmission of concrete. Research conclusions have great significance for predicting the distance of concrete and matching the optimal air supply pressure.

2. Experimental Conditions

2.1. Experimental Apparatus. Two specifications (2.0-inch and 2.5-inch diameter) of concrete conveying lines were set in the pressure drop experiment in the accelerate zone. The feeder used the PTS7 pushing chained shotcrete machine made by Shandong Wit Laboratory Mining Equipment Co., Ltd (Figure 1). The shotcrete machine conveys concrete to the outlet using a piston and achieves the long-distance conveying of concrete via compressed air. This equipment is applicable to dry and wet concrete spraying. The maximum spraying capability of this shotcrete machine was 6 m^3/h. Its theoretical gas consumption and rated wind pressure were 8 m^3/min and 0.5 MPa, respectively. The shotcrete machine motor used the variable-frequency control of speed. The rotating speed of the motor could be adjusted by the transducer, thus controlling concrete throughput during concrete conveying.

The structure of the concrete line is shown in Figure 2, which covers four bent lines. The radius of two of the bent

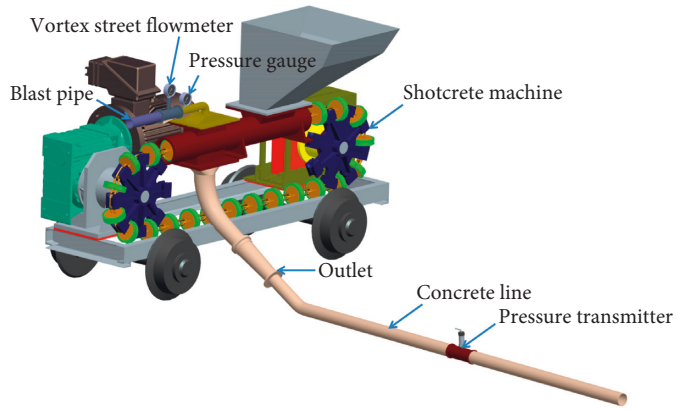

Figure 1: Structure of the PTS7 pushing chained shotcrete machine.

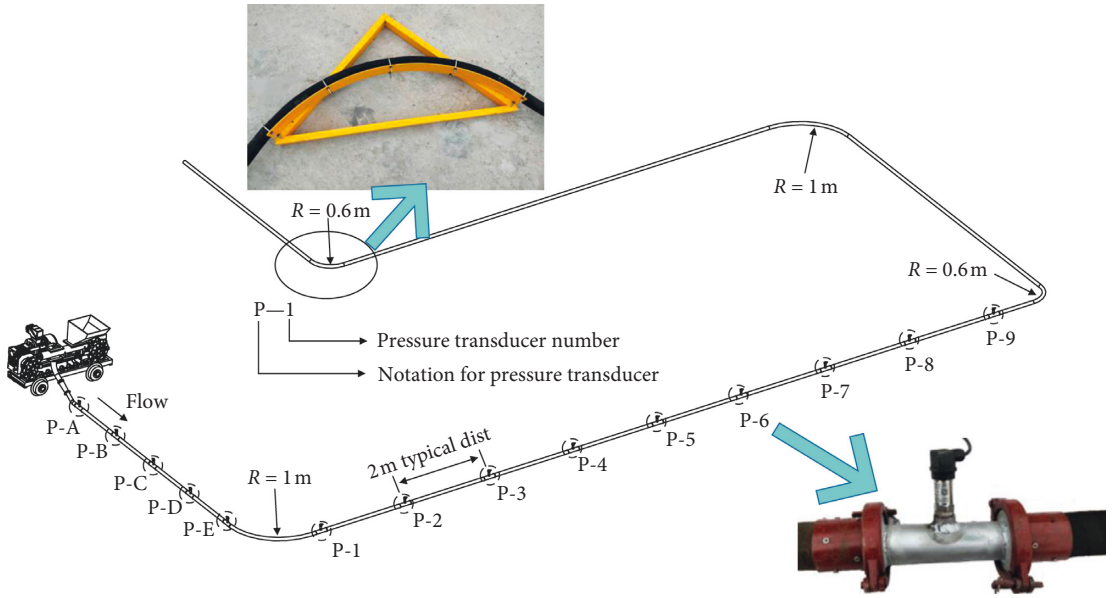

Figure 2: Structure of concrete lines.

lines was 1 m, and the radius of the other two bent lines was 0.6 m. To assure consistency of the concrete lines, the bend of the line was fixed onto the self-made bend fixing device using an ordinary rubber hose. During line pavement, horizontality and coaxial performance of concrete lines were verified by the rotating laser.

2.2. Experimental Instruments. Compressed air enters the shotcrete machine via the regulating valve and vortex shedding flowmeter to adjust and measure the input pressure and flow rate of compressed air. In the present experiment, the pressure drop in the concrete lines was measured by a high-accuracy flat film pressure transmitter. The sensor applied the Dwyer FDT series of the flat film pressure transmitter made by the Deville Company (USA), with a measuring range of 0–1.6 MPa and an accuracy of 0.02%. According to the service manual of the sensor, the pressure transmitter was installed on a section of the specially made line, and the concrete line was fixed onto a rubber hose by a special pipe clamp. To prevent scratches of the sensor by gravels, a strainer was installed before the pressure transmitter (Figure 3).

The temperature and flow rate of the compressed air were measured by a vortex shedding flowmeter. The temperature was viewed as constant throughout the conveying of concrete. Hence, the temperature in the entire line was equal to the inlet temperature. The temperature of the mixed concrete in all experiments was controlled between 15 and 20°C.

The rotating speed of the chain wheel was 20 r/min when the shotcrete machine reached the maximum delivery capacity (6 m^3/h). The feeding speed of the shotcrete machine could be adjusted by a transducer. The vortex shedding flowmeter for measuring the flow rate of compressed air and the pressure transmitter for measuring pressure in the lines were read, and data were received by the paperless recorder.

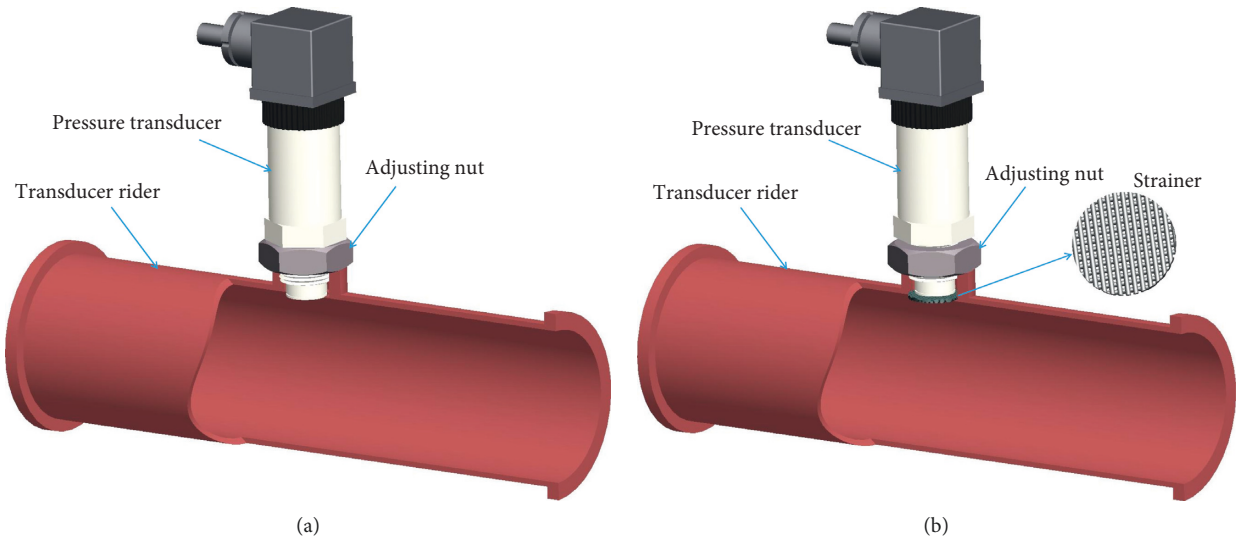

FIGURE 3: Installation structure of the pressure transmitter on lines. (a) Standard installation structure of the pressure transmitter. (b) Installation structure of the pressure transmitter with strainer.

2.3. Experimental Materials

2.3.1. Cement. The cement used in the experiments was PO42.5 cement made by the Shandong Shanshui Cement Group. Its purity and specific gravity were 3100 cm^2/g and 3.14, respectively.

2.3.2. Aggregates. Aggregates can be divided into fine and coarse aggregates. The former used natural river sands. After screening, its fineness modulus, silt content, and apparent density were 2.75, 1.2%, and 2.68 g/cm^3, respectively. The coarse aggregate applied was ordinary limestone fragments whose maximum grain size was less than 10 mm. Continuous grading was performed to remove impurities before mixing the fine and coarse aggregates. The grading curves of fine and coarse aggregates are shown in Figure 4, and they conform to limitations of recommended grades in the national standard GB50086-2001 [27].

2.3.3. Chemical Admixture. The main chemical admixture in this experiment was accelerator. This accelerator was a kind of powdery solid, with density 4 g/cm^3.

2.3.4. Concrete Ratio. In the experiment, the concrete was made up according to the common concrete ratio in the coal mine. Also, the concrete ratio was cement : fine aggregates : coarse aggregates : accelerator = 1 : 2 : 2 : 0.03.

3. Experimental and Analysis Methods

The PTS7 pushing chained shotcrete machine used in the experiments can achieve material feeding at a constant speed by motor-driven piston motion. The prediction of the pressure drop during wind-driven conveying of concrete predicts the pressure drop in unit length. In concrete lines, the acceleration process of concrete mainly distributes at the initial conveying section and after passing the bent line. The effects of these acceleration processes are identical. Therefore, attention was given to the pressure drop during the acceleration processes of concrete in the initial section and after passing the bent line in the experiments.

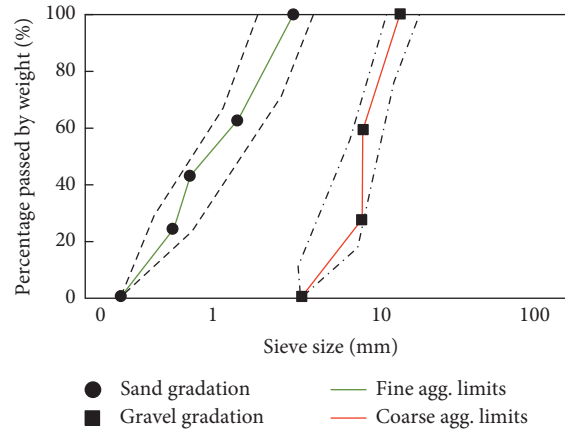

FIGURE 4: Grade curves of fine and coarse aggregates.

In the pressure drop test during concrete conveying, the pressure in the concrete lines must be measured. To prevent scratches on the pressure transmitter from the gravels, the experiment was performed using the following method.

Before the commencement of the experiment, the concrete lines were verified by only supplying compressed air:

(1) Figure 3(a) shows that without the strainer, the bottom of the pressure transmitter was installed onto the inner wall of the concrete lines. The compressed air was supplied, and the pressure at different positions along the line was recorded by pressure transmitters. This is the universal method for the pressure transmitter, and it can accurately measure the pressure in concrete lines.

(2) In Figure 3(b), a strainer was placed on the mounting base of the pressure transmitter. Later, the pressure transmitter was installed to keep the bottom of the pressure transmitter 2 mm away from the strainer. Compressed air was supplied, and pressures along the concrete line were recorded by the pressure transmitter.

Pressures under the above two conditions are summarized in Figure 5. During this process, the pressures at the different positions that were measured by the two methods had a fixed difference of ΔP_0. When the pressure in the concrete conveying was measured by the method in Figure 3(b), the pressure in the concrete line was equal to the sum of the measured pressure P_0 and ΔP_0. In other words, pressure changes after the addition of a strainer could be used to reflect the pressure changes in the concrete lines throughout conveying.

The acceleration pressure drop in the horizontal section of the concrete conveying was mainly caused by the mean pressure difference measured by the pressure transmitter. The measured acceleration pressure drop between any two points in the analysis region was discussed. However, whether concrete was in the initial section or had passed the bent line was neglected; thus, it was believed that the momentum and energy changes were the same given the same velocity changes.

During the experiment, pressure drop in the accelerate zone occurred, as shown in Figure 6. The pressure drop curve shows that the pressure drop in the accelerate zone reached a relatively stable trend. The pressure curve during this process was fitted, and a straight line representing the steady-state pressure drop was deduced based on the final process of the stable pressure drop. Based on this deduced straight line, the pressure at zero speed could be determined.

In Figure 6, $\Delta P_{\text{acctotal}}$ is the total pressure drop in the accelerate zone, and ΔP_{acc} is the acceleration pressure drop of concrete.

According to reverse deduction from the stable value of the above curves, energy loss under steady state can be obtained from the index trend and linear pressure gradient trend of floating points, leading to the acceleration of pressure drop and thus obtaining the actual pressure drop trend. An exponential linear equation was fitted by the pressure fitting curve in Figure 6:

$$P_0 = p_1 \cdot e^{-x/p_2} + p_3 \cdot x + p_4. \quad (3)$$

Here, x is the length of the test section and p_1, p_2, p_3, and p_4 are constants. The numerical value in Figure 6 was brought into equation (3), thus obtaining the following equation:

$$P_0 = 11 \cdot e^{-0.36x} - 45x + 307. \quad (4)$$

This pressure-distance relation equation covers two parts: (1) $p_1 \cdot e^{-x/p_2}$ is the exponential function that reflects the pressure drop caused by the acceleration in the concrete line. (2) $p_3 \cdot x + p_4$ is the linear function that reflects the pressure drop caused by concrete collision and friction in the line. Under this circumstance, the pressure drop is distributed uniformly. Based on the above curves, we can obtain the following results:

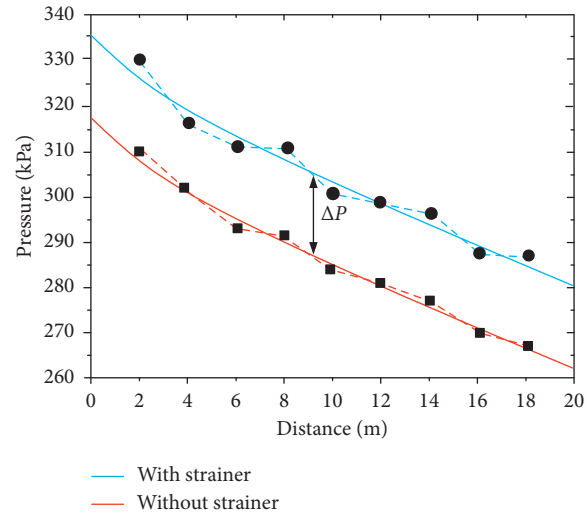

Figure 5: Effects of the strainer in the pressure transmitter on the gas-phase pressure drop.

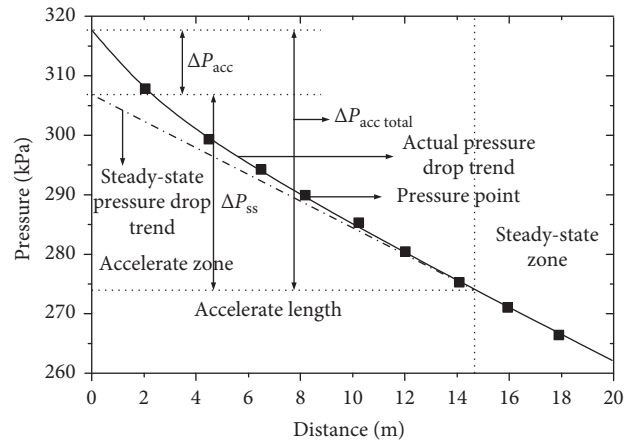

Figure 6: Trend of pressure drop during concrete conveying.

(a) Steady pressure drop in the concrete line.

(b) Accelerated pressure drop in the concrete line.

(c) The pressure at the beginning of acceleration is difficult to measure. Under this circumstance, the pressure at the beginning of acceleration can be deduced by the equation. Thus, the pressure drop from zero to a steady speed could be calculated.

(d) Length of the accelerate zone (part 1 in the equation is approaching zero).

To predict the length of the accelerate zone during concrete conveying, Wei et al. introduced the Archimedes number [28]. The Archimedes number mainly reflects the ratio between buoyancy and viscosity force and can be expressed as

$$\mathrm{Ar} = \frac{(\rho_c - \rho_f) g \cdot d^3}{v^2 \cdot \rho_f}, \tag{5}$$

where Ar is the Archimedes number, ρ_c is the density of concrete, ρ_f is the density of air, v is the kinematic viscosity, and d is the mean diameter of concrete particles.

In the present study, the conveying speed of the concrete particles was measured with a high-speed camera. Pressure changes in the concrete line were measured by the pressure transmitter. The length of the accelerate zone of concrete was expressed by particle speed and pressure changes. Moreover, the relation between the Archimedes number and length of the accelerate zone was expressed as

$$L_{acc} = 1.6\mathrm{Ar}^{0.1}. \tag{6}$$

During the present experiment, the total pressure drop in the accelerate zone was expressed as the sum of steady-state pressure drop and accelerated pressure drop (equation (7)). The accelerated pressure drop (ΔP_{acc}) is the momentum equation of concrete and can be expressed as equation (8).

$$\Delta P_{acctotal} = \Delta P_{ss} + \Delta P_{acc}, \tag{7}$$

$$\Delta P_{acc} = \Delta P_{mom} = \frac{\dot{m}_s \Delta u_c}{A} = \frac{\dot{m}_s (u_{css} - 0)}{A}, \tag{8}$$

where $\Delta P_{acctotal}$ is the total pressure drop of the accelerate zone, ΔP_{acc} is the accelerated pressure drop of concrete, ΔP_{ss} is the constant pressure drop of concrete, and $\dot{m}_s$ is the mass velocity of concrete particle flow.

The total pressure drop in equation (7) was used to calculate the derivation of displacement and can be expressed as

$$\frac{dP_{acctotal}}{dx} = \frac{dP_{ss}}{dx} + \frac{dP_{acc}}{dx}. \tag{9}$$

To analyze the steady-state speed and transient speed during concrete conveying, an equation was constructed in the present experiment with reference to the study by Wei et al. [28]:

$$\frac{u_{css}}{u_f} = 1 - 0.072\left[\mathrm{Ar} \cdot \frac{\rho_c - \rho_f}{v^2 \cdot \rho_f}\right]^{0.091}, \tag{10}$$

$$\frac{u_c}{u_{css}} = 1 - e^{-4.8x/L_{acc}}, \tag{11}$$

where u_{css} is the steady speed of concrete, u_c is the initial velocity of concrete, and u_f is the air velocity. The derivative of distance was calculated based on equation (10) and was brought into equation (11):

$$\frac{dP_{acctotal}}{dx} = \frac{dP_{ss}}{dx} + \frac{\dot{m}_s}{A}\frac{du_c}{dx}. \tag{12}$$

The value of u_c in equation (8) was brought into equation (12) to obtain

$$\frac{dP_{acctotal}}{dx} = \frac{dP_{ss}}{dx} + \frac{\dot{m}_s \cdot u_{css}}{A}\frac{du_c}{dx}\left(1 - e^{-4.8x/L_{acc}}\right). \tag{13}$$

Based on the integration of the displacement x through equation (13), the following was obtained:

$$\int_0^{L_{acc}} \left(\frac{dP_{acctotal}}{dx}\right) dx = \int_0^{L_{acc}} \left(\frac{dP_{ss}}{dx}\right) dx - \int_0^{L_{acc}} \frac{\dot{m}_s \cdot u_{css}}{A}\frac{4.8}{L_{acc}} \left(1 - e^{-4.8x/L_{acc}}\right) dx. \tag{14}$$

Therefore,

$$P_{total} = \frac{\dot{m}_s}{A} u_{css} \cdot e^{-(4.8/L_{acc})x} + p_3 \cdot x + p_4. \tag{15}$$

By comparing equations (3) and (15), the following was obtained:

$$p_1 = \frac{\dot{m}_s}{A} u_{css}, \qquad p_2 = -\frac{4.8}{L_{acc}} x. \tag{16}$$

Thus, the accelerated pressure drop of concrete can be expressed as

$$\Delta P_{acc} = \frac{\dot{m}_s}{A} u_{css} \cdot e^{-(4.8/L_{acc})x} = \frac{\dot{m}_s}{A} u_{css} \cdot e^{-(4.8/1.6\mathrm{Ar}^{0.1})x} = \frac{\dot{m}_s}{A} u_{css} \cdot e^{-\left(4.8/1.6\left(\left((\rho_c - \rho_f) g \cdot d^3\right)/\left(v^2 \cdot \rho_f\right)\right)^{0.1}\right)x}. \tag{17}$$

To protect the accuracy of the conclusions, the concrete flow trend in the constant speed section was verified by changing the supply quantity of concrete and air input. The starting point of the constant speed section was set at 15 m after the bent line. In the experiment, the concrete supply was controlled by the rotating speed of the motor of the transducer. During this process, the relationship between the pressure drop during concrete conveying and concrete supply was found, as shown in Figure 7. The figure shows the effects of air flow and concrete supply quantity on pressure drop during the conveying of concrete.

However, equation (7) focused on testing the physical property of the accelerated pressure drop, which is the relationship between the momentum equation and pneumatic transmission during the conveying of concrete. To accurately predict the relationship of accelerated pressure drop in the conveying of concrete, the correction factor α was introduced to increase the prediction accuracy. Therefore, the prediction of the total pressure drop in the acceleration zone was calculated as

$$\Delta P_{acctotal} = \alpha \Delta P_{ss} + \Delta P_{acc}. \tag{18}$$

4. Results and Discussions

It is very simple to predict the pressure drop during concrete conveying by experiments. First, it must be determined that the pressure drop during concrete conveying is caused by accelerated conveying, friction, and the collision of concretes. The pressure drop caused by the acceleration of

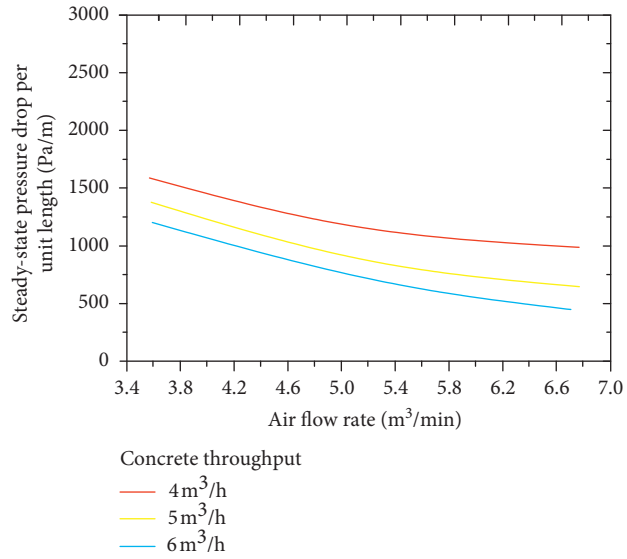

Figure 7: Variations of pressure drop in the constant speed section with air flow.

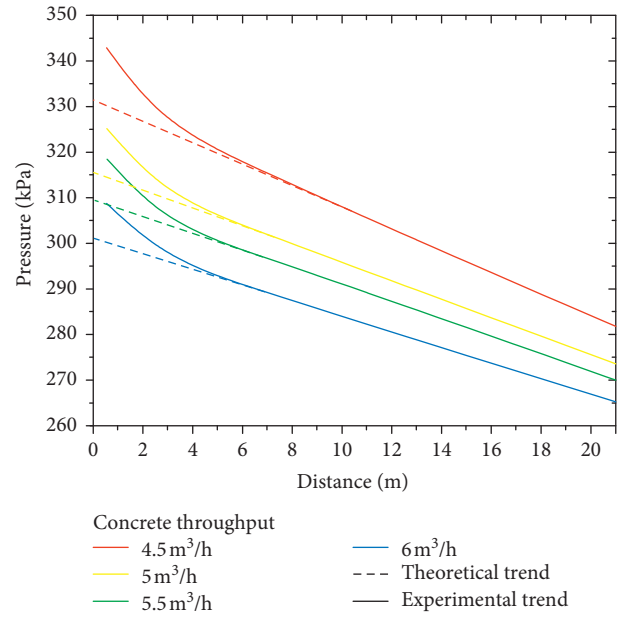

Figure 8: Variation trend of concrete pressure.

concrete is also called the accelerated pressure drop, and it only exists in the accelerate zone. The pressure drop caused by friction and collision is called the uniform pressure drop, and it exists throughout the conveying of concrete. Therefore, the pressure drop caused by acceleration can be calculated by the accelerated pressure drop minus the uniform pressure. In the calculation of pressure drop during concrete conveying, the sum of steady-state pressure drop and accelerated pressure drop is the total pressure drop in the accelerate zone. This relationship is based on the hypothesis that the steady-state pressure drop in the accelerate zone and constant speed section are the same.

When predicting the pressure drop during concrete conveying, the accelerated pressure drop can be predicted by equation (8). Hence, the steady-state speed in the conveying of concrete must be known, which can be calculated by equations (10) and (11). During the present experiment, the rotating speed of the motor was changed by the transducer, thus changing the mass flow rate during concrete conveying. Simultaneously, the pressures at different positions in the accelerate zone and constant speed zone could be measured.

The experimental pressure drop trend of concrete under different mass flow rates is shown in Figure 8, which is comparing the curves drawn based on equation (17). Figure 8 shows that the increasing trend of the curves under different supply quantities of concrete is the same. Based on the comparison of the curves drawn in accordance with Figure 8, the theoretical trend might overlap with the actual curve measured in the experiment. If these two curves overlap, then the actual pressure drop during concrete conveying is similar to the predicted pressure drop, proving the accuracy of the prediction. If the actual pressure drop does not overlap with the predicted pressure drop, the steady-state pressure drop in the accelerate zone is different from that in the constant speed zone.

The effects of concrete pressure (p_0) at the beginning position on the pressure drop trend along the concrete conveying are shown in Figure 9. Normalization of pressure during concrete conveying based on p_0 can decrease the influence of the air flow rate on the pressure measurement, and the maximum error can be controlled within 2%.

During multiple experimental processes, the value of α was calculated by changing the air flow rate and feeding rate of concrete under different motor speeds.

Accelerated pressure drop and uniform pressure drop during the concrete conveying were predicted based on the value of α. If $\alpha = 1$, the pressure drop caused by concrete collision and friction was the same in the constant speed section. If $\alpha < 1$, the pressure drop was relatively small because of the low conveying speed of concrete. In contrast, $\alpha > 1$ indicates a high pressure drop because of the high conveying speed of concrete. In the constant speed section of concrete, particle collision was weak. However, particle collision frequency was high and particle collision was strong in the accelerate zone, resulting in the high energy loss of concrete particles. Therefore, the pressure drop in the accelerate zone was higher than that in the constant speed section.

The difference between the experimental and theoretical results of concrete conveying was positively related to the concrete throughput given the same flow rate of compressed air. When the concrete throughput was small, the experimental results and theoretical results were similar, indicating that α was closer to 1 (Figure 10). With an increase of concrete throughput, the difference of experimental and theoretical results gradually increased. The difference is the key factor influencing the prediction of concrete conveying.

Next, the value of the transducer was fixed, and the concrete was input by the shotcrete machine at a constant feeding rate. Subsequently, pressures at different points were tested by controlling the input of compressed air with the

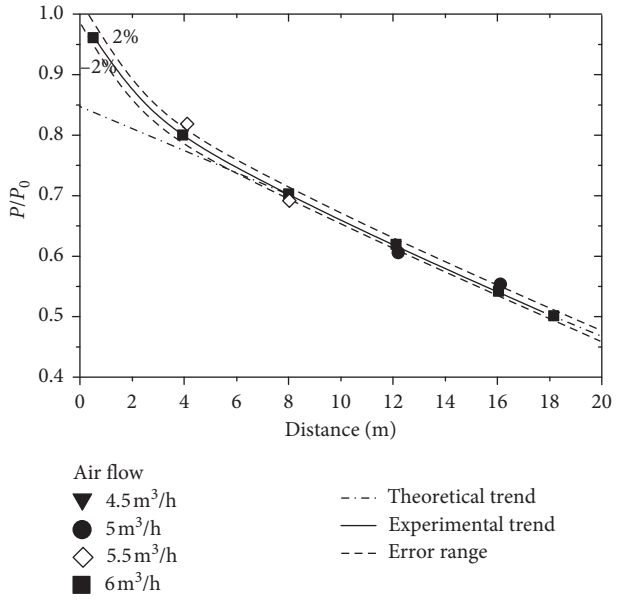

Figure 9: Normalization trend under different wind speeds.

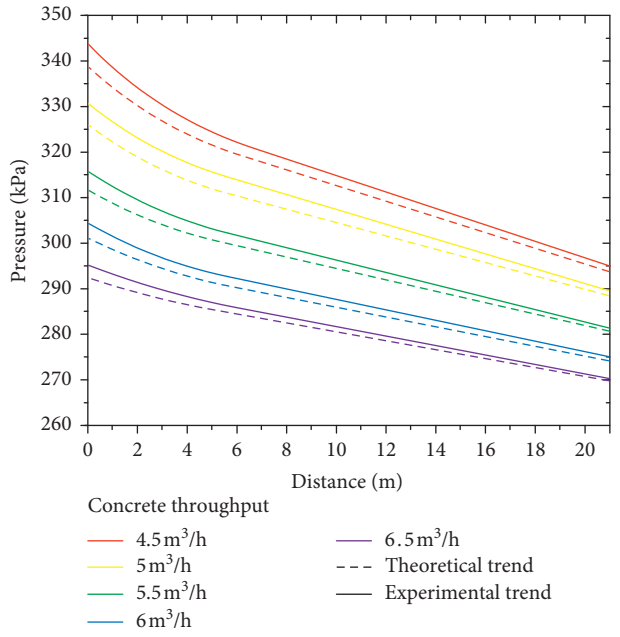

Figure 10: Comparison of theoretical and experimental pressures after adding α.

regulating valve. There was a large difference between the experimental results and theoretical results. With an increase of air flow rate, such differences decreased gradually. This difference was also a key factor that influenced the prediction of concrete conveying.

Figures 10 and 11 show that the value of α had a direct relationship with concrete throughput and input of compressed air. Tripathi et al. tested materials of different grain sizes [29], and α can be defined as

$$\alpha = a + \left(b \cdot e^{-c \cdot \mu}\right), \tag{19}$$

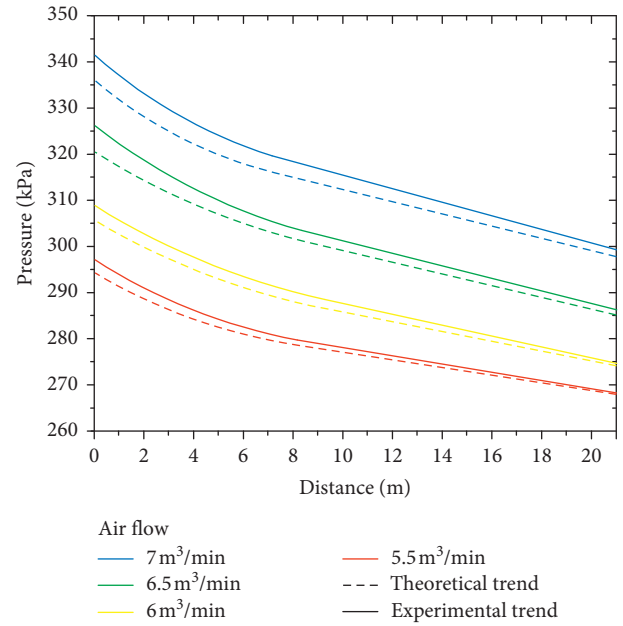

Figure 11: Comparison of pressure drop in the accelerate zone.

where $\mu = m_c/m_f$ is the ratio of concrete mass and air mass.

Experimental data from Figures 11 and 12 were brought into equation (19), yielding the following:

$$\alpha = 1.2 + \left(0.11e^{-0.9\mu}\right). \tag{20}$$

During the accelerated pressure drop experiment, the conveying of concrete particles was accelerated at a specific speed from one point and finally reached the movement trend at a constant speed [30–32]. The momentum equation was used to calculate the pressure drop during this process:

$$\Delta P_{acc} = \Delta P_{mom} = \frac{\dot{m}_s \cdot \Delta u_c}{A} = \frac{\dot{m}_s \cdot \left(u_{css} - u_c\right)}{A}. \tag{21}$$

Pressure drop is at equilibrium in the constant speed section. Therefore, the total accelerated pressure drop can be gained from equations (18), (19), and (21). The total accelerated pressure drop was expressed as

$$\Delta P_{acctotal} = \left[1.2 + \left(0.11e^{-0.9\mu}\right)\right]\Delta P_{ss} + \frac{\dot{m}_s \cdot \left(u_{css} - u_c\right)}{A}. \tag{22}$$

Also, equations (1) and (2) were brought into equation (22), and thus the total accelerated pressure drop was expressed as

$$\Delta P_{acctotal} = \left[1.2 + \left(0.11e^{-0.9\mu}\right)\right]\left(f_D \frac{\rho_f u_f^2}{2D} L + \Delta P_c\right) + \frac{\dot{m}_s \cdot \left(u_{css} - u_c\right)}{A}. \tag{23}$$

To verify the accuracy of equation (20), the feeding rate of concrete was kept constant in the experiment. The concrete-air ratio was changed by altering the air flow rate to analyze the pressure at different positions along the line. Comparison between theoretical and experimental

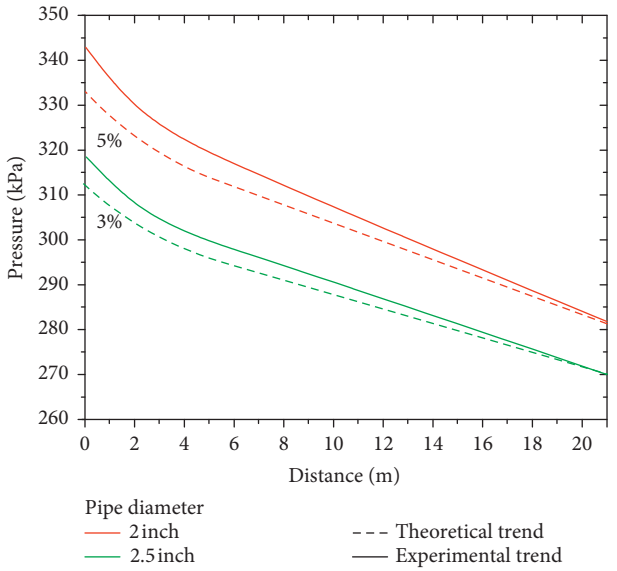

Figure 12: Pressure drop at different specifications of concrete lines.

pressures is shown in Figure 12. The curve equation gained from the theoretical formula was similar to the experimental results, showing a maximum error of less than 10%. This verified the universality of equation (20). In this experiment, pipe diameters of 2.0 inches and 2.5 inches of the concrete line were applied. Pressures at different positions of the concrete line were tested by a pressure transmitter (Figure 12). The maximum error was less than 5%, verifying the feasibility of equation (20).

5. Conclusions

In order to obtain the pressure drop in the accelerate zone of horizontal conveying of concrete spraying, the concrete conveying pipeline was arranged to conduct the related concrete conveying experiment. The concrete was made up, according to the common concrete ratio in the coal mine. Each point pressure on the pipeline during the progress of conveying was tested by the pressure transmitter set up on the pipeline. Also, the pressure drop in the accelerate zone of horizontal conveying of concrete spraying was analyzed with measured pressure.

The results show that the pipeline pressure dropped rapidly at the beginning of the conveying and at the end of the bending pipe, and the trend of the dropping linearly was showed gradually. The accelerated pressure drop was analyzed by combining experimental and momentum equations during concrete conveying. The accelerated pressure drop was analyzed, which was mainly caused by acceleration, friction, and the collision of concretes. Also, the friction and the collision of concretes also exist in the zone of stable convey.

The pressure drop curve was drawn according to the pressure at each point in the concrete conveying process. Also, the mathematical model of pressure drop in the concrete conveying process was set up. To prevent random interference factor from the friction, and the collision, and improving the calculation accuracy, the correction factor α was introduced.

Finally, the measured pressures under different concrete throughputs and flow rates of compressed air were compared with the results from the mathematical model, which verified the accuracy of the mathematical model. Also, the main factors of pressure drop in the accelerate zone were obtained as the ratio of the concrete mass and the compressed mass, the initial velocity of the concrete, the optimal final required velocity, the feed speed of concrete, and cross section area of the conveying pipeline.

Data Availability

The data used to support the findings of this study are available from the corresponding author upon request.

Additional Points

Innovations and highlights: (1) Damage to the pressure transmitter by concrete can be prevented by installing a strainer before the pressure transmitter. (2) Variation laws of pressure before and after the installation of a pressure transmitter were studied by supplying air only. (3) A statistical analysis of the pressures at different positions along the concrete conveying line under different input quantities of concrete and compressed air was performed. Based on this, the law of pressure drop during the conveying of concrete was discussed. (4) The pressure drop in the line during the conveying of concrete was predicted.

Conflicts of Interest

The authors declare that they have no conflicts of interest.

References

[1] L. Chen, G. Liu, W. Cheng, and G. Pan, "Pipe flow of pumping wet shotcrete based on lubrication layer," *SpringerPlus*, vol. 5, no. 1, p. 945, 2016.

[2] Y. Cai, Y. Jiang, I. Djamaluddin, T. Iura, and T. Esaki, "An analytical model considering interaction behavior of grouted rock bolts for convergence-confinement method in tunneling design," *International Journal of Rock Mechanics and Mining Sciences*, vol. 76, pp. 112–126, 2015.

[3] L. Chen, P. Li, G. Liu, W. Cheng, and Z. Liu, "Development of cement dust suppression technology during shotcrete in mine of China-a review," *Journal of Loss Prevention in the Process Industries*, vol. 55, pp. 232–242, 2018.

[4] L. Chen and G. Liu, "Airflow-dust migration law and control technology under the simultaneous operations of shotcreting and drilling in roadways," *Arabian Journal for Science and Engineering*, vol. 44, no. 5, pp. 4961–4969, 2019.

[5] Q. Liu, W. Nie, Y. Hua, H. Peng, and Z. Liu, "The effects of the installation position of a multi-radial swirling air-curtain generator on dust diffusion and pollution rules in a fully-mechanized excavation face: a case study," *Powder Technology*, vol. 329, pp. 371–385, 2018.

[6] R. Naveh, N. M. Tripathi, and H. Kalman, "Experimental pressure drop analysis for horizontal dilute phase particle-fluid flows," *Powder Technology*, vol. 321, pp. 353–368, 2017.

[7] O. G. Brown, "The history of the Darcy-Weisbach equation for pipe flow resistance," in *Proceedings of the Environmental and Water Resources History*, pp. 34–43, Washington, DC, USA, November 2003.

[8] O. Molerus, "Overview: pneumatic transport of solids," *Powder Technology*, vol. 88, no. 3, pp. 309–321, 1996.

[9] Q. Liu, W. Nie, Y. Hua, H. Peng, C. Liu, and C. Wei, "Research on tunnel ventilation systems: dust diffusion and pollution behaviour by air curtains based on CFD technology and field measurement," *Building and Environment*, vol. 147, pp. 444–460, 2019.

[10] Y.-Q. Zhang, J.-L. Zhu, X.-H. Wang, X.-W. Zhang, S.-X. Zhou, and P. Liang, "Simulation of large coal particles pyrolysis by circulating ash heat carrier toward the axial dimension of the moving bed," *Fuel Processing Technology*, vol. 154, pp. 227–234, 2016.

[11] Y. Tomita, H. Tashiro, K. Deguchi, and T. Jotaki, "Sudden expansion of gas-solid two-phase flow in a pipe," *Physics of Fluids*, vol. 23, no. 4, pp. 663–666, 1980.

[12] P. Li, Z. Zhou, L. Chen, G. Liu, and W. Xiao, "Research on dust suppression technology of shotcrete based on new spray equipment and process optimization," *Advances in Civil Engineering*, vol. 2019, Article ID 4831215, 11 pages, 2019.

[13] B. Kong, E. Wang, and Z. Li, "The effect of high temperature environment on rock properties—an example of electromagnetic radiation characterization," *Environmental Science and Pollution Research*, vol. 25, no. 29, pp. 1–11, 2018.

[14] A. Shimizu, R. Echigo, S. Hasegawa, and M. Hishida, "Experimental study on the pressure drop and the entry length of the gas-solid suspension flow in a circular tube," *International Journal of Multiphase Flow*, vol. 4, no. 1, pp. 53–64, 1978.

[15] N. Guanhua, D. Kai, L. Shang, and S. Qian, "Gas desorption characteristics effected by the pulsating hydraulic fracturing in coal," *Fuel*, vol. 236, pp. 190–200, 2019.

[16] G. Zhou, Y. Ma, T. Fan, and G. Wang, "Preparation and characteristics of a multifunctional dust suppressant with agglomeration and wettability performance used in coal mine," *Chemical Engineering Research and Design*, vol. 132, pp. 729–742, 2018.

[17] R. D. Marcus, J. D. Hilbert Jr., and G. E. Klinzing, "Flow through bends and acceleration zones in pneumatic conveying systems," *Bulk Solids Handling*, vol. 5, no. 4, pp. 121–126, 1985.

[18] T. Fan, G. Zhou, and J. Wang, "Preparation and characterization of a wetting-agglomeration-based hybrid coal dust suppressant," *Process Safety and Environmental Protection*, vol. 113, pp. 282–291, 2018.

[19] R. A. Duckworth, *Empirical Correlations For The Dilute Phase*, Department of Chemical Engineering, The University of Queensland, Brisbane, Australia, Lecture notes C.S.I.R.O. Mineral engineering, 1969.

[20] Y. Tomita and H. Tashiro, "Loss coefficient for abrupt enlargement in pneumatic transport of solids in pipes," *Bulk Solid Handling*, vol. 8, pp. 129–131, 1988.

[21] J. A. Ottjes, "Digital simulation of pneumatic particle transport," *Chemical Engineering Science*, vol. 33, no. 6, pp. 783–786, 1978.

[22] H. V. Nguyen, R. Yokota, G. Stenchikov et al., "A parallel direct numerical simulation of dust particles in a turbulent flow," in *Proceedings of the EGU General Assembly Conference Abstracts*, Vienna, Austria, April 2012.

[23] N. Huber and M. Sommerfeld, "Modelling and numerical calculation of dilute-phase pneumatic conveying in pipe systems," *Powder Technology*, vol. 99, no. 1, pp. 90–101, 1998.

[24] K. J. Hanley, E. P. Byrne, and K. Cronin, "Probabilistic analysis of particle impact at a pipe bend in pneumatic conveying," *Powder Technology*, vol. 233, pp. 176–185, 2013.

[25] G. E. Klinzing and O. M. Basha, "A correlation for particle velocities in pneumatic conveying," *Powder Technology*, vol. 310, pp. 201–204, 2017.

[26] H. G. Merkus and G. M. H. Meesters, "Production, handling and characterization of particulate materials," *Particle Technology*, vol. 11, no. 4, pp. 619–629, 2016.

[27] G. Liu, W. Cheng, and L. Chen, "Investigating and optimizing the mix proportion of pumping wet-mix shotcrete with polypropylene fiber," *Construction and Building Materials*, vol. 150, pp. 14–23, 2017.

[28] W. Wei, G. Qingliang, W. Yuxin, Y. Hairui, Z. Jiansheng, and L. Junfu, "Experimental study on the solid velocity in horizontal dilute phase pneumatic conveying of fine powders," *Powder Technology*, vol. 212, no. 3, pp. 403–409, 2011.

[29] N. M. Tripathi, A. Levy, and H. Kalman, "Acceleration pressure drop analysis in horizontal dilute phase pneumatic conveying system," *Powder Technology*, vol. 327, pp. 43–56, 2018.

[30] L. Chen, G. Ma, G. Liu, and Z. Liu, "Effect of pumping and spraying processes on the rheological properties and air content of wet-mix shotcrete with various admixtures," *Construction and Building Materials*, vol. 225, pp. 311–323, 2019.

[31] L. Chen and G. Liu, "Airflow-dust migration law and control technology under the simultaneous operations of shotcreting and drilling in roadways," *Arabian Journal for Science and Engineering*, vol. 44, no. 5, pp. 4961–4969, 2019.

[32] B. Kong, E. Wang, W. Lu, and Z. Li, "Application of electromagnetic radiation detection in high-temperature anomalous areas experiencing coalfield fires," *Energy*, vol. 189, Article ID 116144, 2019.